Path-Following Control of an AUV: A Multiobjective Model Predictive Control Approach

Chao Shen, *Member, IEEE*, Yang Shi, *Fellow, IEEE*, and Brad Buckham, *Member, IEEE*

***Abstract*— The path-following (PF) problem of an autonomous underwater vehicle (AUV) is studied, in which the path convergence is viewed as the main task while the speed profile is also taken into consideration as a secondary task. To accommodate the prioritized PF tasks, a novel multiobjective model predictive control (MPC) (MOMPC) framework is developed. Two methods, namely, weighted sum (WS) and lexicographic ordering, are investigated for solving the MOMPC PF problem. A logistic function is proposed for the WS method in an attempt to automatically select the appropriate weights. The Pontryagin minimum principle is subsequently applied for the WS-MOMPC implementation. The implicit relation between the two methods is shown, and the convergence of the solution with the MOMPC PF control algorithms is analyzed. Simulation studies on the Saab SeaEye Falcon AUV demonstrate the effectiveness of the proposed MOMPC PF control.**

***Index Terms*— Autonomous underwater vehicle (AUV), multiobjective MPC (MOMPC), PF control, weighted sum (WS), logistic function, lexicographic ordering (LO).**

I. Introduction

DRAMATIC progress in underwater robotics has resulted in advanced tools for various oceanic missions. The autonomous underwater vehicle (AUV) exemplifies the recent advances. The path-following (PF) control is a fundamental motion control problem for AUVs and finds many real-world applications such as oceanographic survey and pipeline inspection. The design of PF controller is quite complicated and much research effort has been devoted to this topic [1]–[3]. The work reported in [4] presents a powerful PF control structure for land robots. The control structure, however, exploits the kinematic characteristics only. The techniques therein cannot be directly applied to AUVs. Encarnacao and Pascoal [5] took advantage of the backstepping technique and recursively designed the PF controller for the underwater vehicle. Encarnacao *et al.* [6] considered more practical scenarios and provided the PF controller design considering disturbances from ocean currents. However, the controllers in [5] and [6] were designed based on the assumption that the target point is the closest point on the path relative to the vehicle; hence, these methods share an inherent limitation: there exist singularities for certain initial positions of the vehicle, located exactly at the centers of path curvature. To solve this serious problem, Lapierre and Soetanto [7] proposed a novel PF control strategy. The target point is a virtual particle moving along the path and possessing independent dynamic properties. The novel strategy essentially creates an extra degree of freedom (DOF) which could be exploited to achieve additional specifications such as a desired speed assignment. Lapierre and Jouvencel [8] followed this new strategy and developed a robust PF controller by involving an adaption scheme to deal with the parametric uncertainties. Unfortunately, the preceding PF controller designs have no capability to handle system constraints. Accommodating such constraints has been the focus of recent studies of model predictive control (MPC) for PF problems [9]–[11].

The MPC is an optimization-based control strategy which presents a flexible framework to accommodate the complicated system dynamics and nonlinear system constraints. In the context of PF control, there exist several pieces of notable work in the literature. In [12], the PF problem was studied and the MPC was used to optimize the look-ahead distance in the line-of-sight (LOS) guidance law. In [13], a complete linear MPC structure was developed for the LOS-based PF control rather than just adding an optimization of the lookahead parameter. However, the LOS guidance law can only be used to follow straight lines. For general curved paths Faulwasser *et al.* [9] formulated the PF control problem into the MPC framework with an augmented system consisting of the vehicle dynamics and the path dynamics. Sufficient stabilizing conditions were derived. An extended work in terms of output MPC was presented in [10]. The proposed PF controllers in [9] and [10], however, only guarantee a nonzero forward motion and cannot easily accommodate a desired speed assignment. In view of this point, the incorporation of the speed assignment was particularly focused in [14]. The PF task can also be accomplished with a trajectory tracking controller by explicitly assigning a timing law to the path dynamics [15], [16]. In this way, however, the flexibility of adjusting the velocity of the vehicle for possible better path following performance is lost. In practice, an AUV PF controller always prioritizes the path convergence over the speed assignment, and the framework proposed in [14] provides no flexibility to adjust the relative priorities between the path convergence and speed assignment. To address this issue we investigate the multiobjective MPC (MOMPC) method.

The MOMPC has been receiving increasing attentions from the system control community because many practical applications involve meaningful multiple control objectives.

Manuscript received October 30, 2017; accepted December 20, 2017. Date of publication January 23, 2018; date of current version April 11, 2019. Manuscript received in final form January 1, 2018. Recommended by Associate Editor M. Maggiore. This work was supported in part by the Natural Sciences and Engineering Research Council of Canada and in part by the National Natural Science Foundation of China under Grant 61473116. *(Corresponding author: Yang Shi.)*

The authors are with the Department of Mechanical Engineering, Institute for Integrated Energy Systems (IESVic), University of Victoria, Victoria, BC V8W 2Y2, Canada (e-mail: shenchao@uvic.ca; yshi@uvic.ca; bbuckham@uvic.ca).

Color versions of one or more of the figures in this paper are available online at http://ieeexplore.ieee.org.

Digital Object Identifier 10.1109/TCST.2018.2789440

Early results in MOMPC mainly focus on the appropriate problem formulation [17], [18]. In recent years, the MOMPC studies begin to emphasize the closed-loop properties such as stability and optimality. Bemporad and Pena [19] adopted the weighted sum (WS) method and guaranteed the closed-loop stability for a special class of linear systems by adding an intermediate procedure to determine appropriate weights. In [20], the utopia-tracking strategy was employed for the MOMPC problem. By constructing the partial Lagrange function and under assumptions of strong duality and Lipschitz continuity, the utopia-tracking cost can be exploited to establish the nonincreasing property, which guaranteed the closed-loop stability. Another treatment of solving the multiobjective optimization called lexicographic ordering (LO) was adopted in [21]. The optimal value function for the most important objective can be shown a valid Lyapunov function for the closed-loop system. An interesting variant in terms of switched cost MPC was proposed in [22]. The average dwell time was imposed between switches to guarantee the monotonic decrease of the optimal cost over time.

The MOMPC owns an enlarged capacity and potentially handles the objective prioritization in the PF control. In this brief, we develop a novel MOMPC framework for AUVs to solve the PF problem where the objective prioritization can be incorporated. Regarding the competing control objectives, the WS method and the LO method are investigated. For the WS-MOMPC method, a logistic function is introduced for the selection of weights. The Pontryagin minimum principle (PMP) is then applied for fast implementation. For the LO-MOMPC method, the controller design that guarantees the path convergence is provided explicitly. The internal relationship between the two methods is also explored. The main contributions of this brief include the following.

1) A novel MOMPC framework is developed for the AUV PF problem, in which the prioritized PF tasks can be explicitly considered.
2) The WS and LO methods are proposed to solve the problem; the implicit relation between the two methods is shown from the optimization perspective.
3) A novel logistic function is introduced to deal with the weights associated with the WS-MOMPC method; and with several properly defined barrier functions, the PMP is applied to the WS-MOMPC implementation.
4) Sufficient conditions that guarantees the convergence of the solution under the MOMPC algorithms are derived; and a feasible way to satisfy the conditions is provided for the LO-MOMPC implementation.

The remainder of this brief is organized as follows. Section II introduces the AUV system model. In Section III, the MOMPC formulation is provided. Two methods that solve the formulated MOMPC problem are proposed in Section IV. Section V derives the conditions that guarantee the convergence of the solution. In Section VI, the simulation results are presented and in Section VII several conclusive remarks are pointed out.

Notations: The column operation $[\rho_1^T, \dots \rho_n^T]^T$ is written as $col(\rho_1, \dots, \rho_n)$; diagonal operation is abbreviated by $\mathrm{diag}(\cdot)$; and the weighted norm $(\rho^{\mathrm{T}} Q \rho)^{1/2}$ is denoted by $\|\rho\|_Q$. For a function $p(s)$ the derivative with respect to s is represented as $p'(s)$ while the time derivative is denoted by $\dot{p}(s)$.

II. AUV System Modeling

In this brief, we study the motion of a fully actuated AUV in the local level plane. Following the standard practice in modeling marine vehicles [23], the kinematic equations of the AUV motion can be modeled by:

$$\begin{aligned} \dot{x} &= u\cos\psi - v\sin\psi \\ \dot{y} &= u\sin\psi + v\cos\psi \\ \dot{\psi} &= r \end{aligned} \tag{1}$$

where $\boldsymbol{\eta} = [x, y, \psi]^{\mathrm{T}}$ denotes the pose of the AUV represented in the inertial reference frame and $\mathbf{v} = [u, v, r]^{\mathrm{T}}$ denotes the velocities of the vehicle represented in body reference frame.

The dynamic equations of motion can be expressed as

$$\begin{aligned} \dot{u} &= \frac{M_{\dot{v}}}{M_{\dot{u}}} vr - \frac{X_u}{M_{\dot{u}}} u - \frac{D_u}{M_{\dot{u}}} u|u| + \frac{F_u}{M_{\dot{u}}} \\ \dot{v} &= -\frac{M_{\dot{u}}}{M_{\dot{v}}} ur - \frac{Y_v}{M_{\dot{v}}} v - \frac{D_v}{M_{\dot{v}}} v|v| + \frac{F_v}{M_{\dot{v}}} \\ \dot{r} &= \frac{M_{\dot{u}} - M_{\dot{v}}}{M_{\dot{r}}} uv - \frac{N_r}{M_{\dot{r}}} r - \frac{D_r}{M_{\dot{r}}} r|r| + \frac{F_r}{M_{\dot{r}}} \end{aligned} \tag{2}$$

where $\boldsymbol{\tau} = [F_u, F_v, F_r]^{\mathrm{T}}$ represents thrust forces and moments; $M_{\dot{u}}$, $M_{\dot{v}}$, and $M_{\dot{r}}$ are inertial coefficients, while X_u, Y_v, N_r and D_u, D_v, D_r are hydrodynamic coefficients corresponding to the linear terms and quadratic terms.

Binding (1) and (2) and defining state $\mathbf{x} = \mathrm{col}(\boldsymbol{\eta}, \mathbf{v})$ and control $\mathbf{u} = \boldsymbol{\tau}$, we can establish the AUV model for the PF control

$$\dot{\mathbf{x}} = f(\mathbf{x}, \mathbf{u}). \tag{3}$$

Since we aim to design an MPC-based PF controller, the continuous-time model (3) needs to be discretized and represented as $\mathbf{x}_{k+1} = f_d(\mathbf{x}_k, \mathbf{u}_k)$.

III. Model Predictive Path-Following Control

Consider a path defined in the d-dimensional output space

$$\mathcal{P} = \{\bar{p} \in \mathbb{R}^d \mid \bar{p} = p(s), \quad s \in [s_0, s_1]\} \tag{4}$$

where s is known as the path parameter with closed but maybe unbounded domain, i.e., $s_1 = +\infty$. The mapping p is assumed to be smooth and bounded. The path $\mathcal{P}$ can be interpreted as the output of the path dynamics governed by

$$\dot{s} = g(s, v_s), \quad \bar{p} = p(s) \tag{5}$$

where v_s is the control input for the path dyanmics.

The output path (4) implicitly defines a zero-path-parameter (ZPE) manifold in the state space

$$s \mapsto p_{\mathbf{x}}(s, \dot{s}, \ddot{s}, \dots) \in \mathbb{R}^n, \quad s \in [s_0, s_1] \subset \mathbb{R}. \tag{6}$$

Then the PF problem can be defined as to determine the control signal $\mathbf{u}(t)$ such that the following requirements are met.

1) *Path Convergence:* The AUV system states converge to the ZPE manifold

$$\lim_{t\to\infty} \|\mathbf{x}(t) - p_{\mathbf{x}}(s(t), \dot{s}(t), \dots)\| = 0 \tag{7}$$

2) *Forward Motion:* The AUV follows the path in the direction of $\dot{s} \geq 0$.
3) *Speed Assignment:* When moving along the path, the desired speed profile is pursued: $\dot{s} \to \dot{s}_r$.
4) *Constraint Satisfaction:* The system constraints such as thrust limits are always satisfied.

Here, the path convergence is identified as the primary task which has to be guaranteed, and the speed assignment is considered as the secondary task that can be sacrificed at times, in lieu of better performance on the primary one.

To establish the MOMPC formulation for the PF problem, we need to find a parametrization of the ZPE manifold. Consider the following desired path in the local level plane:

$$\mathcal{P} = \{\bar{p} \in \mathbb{R}^2 \mid \bar{p} = [p_x(s), p_y(s)]^{\mathrm{T}}, \quad s \in [s_0, s_1]\}. \tag{8}$$

Regarding the kinematic equations (1), we choose the surge velocity u always tangent to the path. Then, the ZPE manifold can be explicitly parameterized as follows:

$$p_{\mathbf{x}}(s, \dot{s}) = [p_x(s), p_y(s), p_\psi(s), p_u(s, \dot{s}), p_v(s), p_r(s, \dot{s})]^{\mathrm{T}}$$

$$p_\psi(s) = \operatorname{atan2}(p_y', p_x'), \quad p_u(s, \dot{s}) = \sqrt{p_x'^2 + p_y'^2}\dot{s} \tag{9a}$$

$$p_v(s) = 0, \quad p_r(s, \dot{s}) = \frac{p_x' p_y'' - p_y' p_x''}{p_x'^2 + p_y'^2}\dot{s}. \tag{9b}$$

Note that above parametrization does not describe the entire manifold implicitly defined by the path (8) but a subset of the ZPE manifold which is simple to be parameterized since we have additionally confined the velocity of the vehicle. However, this is important because the output path (8) only defines the desired position and leaves the yaw angle a DOF. To formulate the PF control into the MPC framework, the reference states have to be uniquely determined.

Considering that only the first-order time derivative is used in the manifold (9a), we simply use a single integrator to describe the path dynamics, i.e.,

$$\dot{s} = g(s, v_s) = v_s \tag{10}$$

which actually facilitates the implementation of the following WS-MOMPC algorithm.

Basically, the AUV PF problem contains two aspects, i.e., path convergence and speed assignment. The path convergence requires the AUV to converge to $\mathcal{P}$ as fast as possible, while the speed assignment requires the path parameter to move in a preferred pace. Since $\dot{s}_r$ is known, stringent fulfilment of the speed assignment results in the determined reference states $p_{\mathbf{x}}(s_r, \dot{s}_r)$ at each time instant. This substantially degrades the PF problem to a trajectory tracking problem where the flexibility of adjusting forward speed may be lost. To maintain the flexibility, the MOMPC can be applied. Consider the following multiobjective optimization problem:

$$\min_U \ J(U, \xi) \tag{11a}$$

$$\text{s.t. } \xi_{k+1} = h(\xi_k, \omega_k), \quad \xi_0 = \xi$$
$$\xi_k \in \Xi, \quad k = 1, 2, \ldots, N$$
$$\omega_k \in \Omega, \quad k = 0, 1, \ldots, N-1 \tag{11b}$$

where $\xi = \operatorname{col}(\mathbf{x}, s)$, $\omega = \operatorname{col}(\mathbf{u}, v_s)$, and $h(\xi, \omega) = \operatorname{col}(f_d, g_d)$ representing the discretized augmented system; $J(U, \xi) = [J_1(U, \xi), J_2(U, \xi)]^{\mathrm{T}}$ is a vector-valued objective function constructed for the two conflicting PF requirements; $U = \operatorname{col}(\omega_0, \omega_1, \ldots, \omega_{N-1})$ is the sequence of control inputs to be optimized; ξ_k denotes the k-step predicted state from initial condition $\xi_0 = \xi$; Ξ and Ω represent the constraints on state and input, respectively. Each objective function has the following form:

$$J_i(U, \xi) = \sum_{k=0}^{N-1} L_i(\xi_k, \omega_k) + E_i(\xi_N) \tag{12}$$

$$L_1(\xi, \omega) = \|\xi - \xi_p\|_{Q_1}^2 + \|\omega\|_{R_1}^2, \quad E_1(\xi) = \|\xi - \xi_p\|_{P_1}^2 \tag{13a}$$

$$L_2(\xi, \omega) = \|\xi - \xi_t\|_{Q_2}^2 + \|\omega\|_{R_2}^2, \quad E_2(\xi) = \|\xi - \xi_t\|_{P_2}^2 \tag{13b}$$

Here, $\xi_p = \operatorname{col}(p_{\mathbf{x}}(s), s)$ can be viewed as the reference for path convergence while $\xi_t = \operatorname{col}(p_{\mathbf{x}}(s_r), s_r)$ is the reference for speed assignment with s_r generated by integrating $\dot{s}_r$ from s_0; Q_i, R_i, and P_i are weighting matrices, positive definite.

IV. Solve the MOMPC Problem

A. Weighted Sum Method

The WS method scalarizes the vector-valued objective function by assigning a weight to each objective. Instead of solving (11), the WS method solves the following single objective problem:

$$\min_U \ J_W = a^{\mathrm{T}} J(U, \xi)$$
$$\text{s.t. (11b)} \tag{14}$$

where $a = [\alpha, 1-\alpha]^{\mathrm{T}}$ with $0 \leq \alpha \leq 1$. Here, we propose a heuristic to choose the appropriate weight α automatically. Consider the following logistic function:

$$\alpha(Er) = \frac{1}{1 + e^{-\beta Er}} \tag{15}$$

where $\mathrm{Er} = \|\boldsymbol{\eta} - \boldsymbol{\eta}_p\|_K^2$ with $\boldsymbol{\eta}_p = [p_x(s), p_y(s), p_\psi(s)]^{\mathrm{T}}$, serves as an indicator of path convergence; $\beta > 0$ controls the change rate of the function; and K is the weighting matrix, positive definite.

Remark 1: The logistic function (15) is smooth and monotonic. By definition the indicator Er is greater than or equal to zero, i.e., the domain of the function is $[0, +\infty)$, then the range is $[0.5, 1)$. Presume that the priority of each objective is positively correlated to the weight, the (15) presents an appropriate choice as the path convergence is prioritized.

We have selected the path dynamics to be a single integrator (10), therefore, the forward motion requirement can be formulated as constraints on the input of the augmented system. Together with AUV thrust limits, we have the input constraint set Ω polyhedral

$$\Omega = \{\omega \in \mathbb{R}^4 \mid \underline{\omega}(j) \leq \omega(j) \leq \bar{\omega}(j), \quad j = 1, \ldots, 4\} \tag{16}$$

Algorithm 1 (WS-MOMPC PF Algorithm)

1: Input the objective functions $J_i(U,\xi)$ in (12).
2: Measure current state $\xi(t)$.
3: Evaluate the value of (15) using $Er(t)$.
4: Solve the PMP conditions (17) with $\xi=\xi(t)$.
5: Let $U^*=col(\omega_0^*,...,\omega_{N-1}^*)$ denote the solution.
6: Implement ω_0^* to the real system.
7: At next time instant, set $t=t+\Delta t$; repeat from step 2.

where $\underline{\omega}(j)$ and $\bar{\omega}(j)$ represent the lower and upper bounds of the jth component. Suppose $s_0=0$ and $s_1=+\infty$, and there is no constraint on the system state, i.e., $\Xi=\mathbb{R}^4$. The scalarized problem (14) can be solved by applying the PMP with the help of several barrier functions. Define the Hamiltonian by

$$\begin{aligned} H(\xi,\lambda,\omega) &= \ell(\xi,\omega)+\lambda^{\mathrm{T}}h(\xi,\omega)-\gamma\left(b_1(\omega)+b_2(\omega)\right)\\ \ell(\xi,\omega) &= \alpha L_1(\xi,\omega)+(1-\alpha)L_2(\xi,\omega)\\ b_1(\omega) &= \sum_{j=1}^{4}\log(\omega(j)-\underline{\omega}(j)),\\ b_2(\omega) &= \sum_{j=1}^{4}\log(\bar{\omega}(j)-\omega(j)). \end{aligned}$$

Here, λ is called the costate and $b_1(\omega)$, $b_2(\omega)$ are barriers for the inequality (16); α is determined by (15) and γ is a small positive number. Define $E(\xi)=\alpha E_1(\xi)+(1-\alpha)E_2(\xi)$, then PMP claims that for a local optimal control $\{\omega_i^*\}_{i=0}^{N-1}$, there exist $\{\lambda_i^*\}_{i=0}^{N}$ satisfying the following conditions:

$$\xi_{k+1}^* = h\left(\xi_k^*,\omega_k^*\right) \tag{17a}$$
$$\lambda_i^* = \lambda_{i+1}^*+H_\xi^{\mathrm{T}}\left(\xi_i^*,\lambda_{i+1}^*,\omega_i^*\right)\Delta t \tag{17b}$$
$$\lambda_N^* = E_\xi^{\mathrm{T}}\left(\xi_N^*\right) \tag{17c}$$
$$\xi_0^* = \xi \tag{17d}$$
$$H_\omega\left(\xi_i^*,\lambda_{i+1}^*,\omega_i^*\right)=0 \tag{17e}$$

which sufficiently solves the Karush–Kuhn–Tucker (KKT) conditions by imposing N boundary conditions (17b) and (17c). Observe that given the initial state ξ and a control input $U=\mathrm{col}(\omega_0,\ldots,\omega_{N-1})$, the states $\{\xi_i^*\}_{i=0}^{N}$ and costates $\{\lambda_i^*\}_{i=0}^{N}$ can be determined via recurrence relations (17a) and (17b). Therefore, we only need to solve (17e), which avoids expensive numerical operations in terms of successive linearizations. Furthermore, fast algorithms based on PMP such as C/GMRES [16] and Gradient Projection [24] can in principle be used.

The WS-MOMPC algorithm is summarized in Algorithm 1.

B. Lexicographic Ordering Method

The WS method is an indirect method which presumes that the value of each objective function at the optimal solution is negatively correlated to its weight. The nonlinear problem (14), however, only guarantees a local minimum, which makes the negative correlation not strictly monotonic. Therefore, a direct method called LO is also studied for the MOMPC PF problem.

To solve the MOMPC problem (11), LO creates a procedure that considers the two objectives, one at a time, ordered by the priority, i.e., at each sampling time instant the following optimizations are solved sequentially:

$$J_1^*(\xi)=\min_U\{J_1(U,\xi)\mid (11\mathrm{b})\} \tag{18a}$$
$$J_2^*(\xi)=\min_U\{J_2(U,\xi)\mid (11\mathrm{b}),\ J_1(U,\xi)=J_1^*(\xi)\}. \tag{18b}$$

Then we obtain the solution for the multiobjective problem

$$U^*=\arg\min_U\{J_2(U,\xi)\mid (11\mathrm{b}),\quad J_1(U,\xi)=J_1^*(\xi)\} \tag{19}$$

Often, to prevent the numerical algorithm from stalling and to improve the computational efficiency, the equality constraint $J_1(U,\xi)=J_1^*(\xi)$ can be relaxed as follows:

$$J_1(U,\xi)\le J_1^*(\xi)+\epsilon \tag{20}$$

where $\epsilon\ge 0$ is a tuning parameter.

The LO method and WS method are closely related. To explore the internal relationship, we simplify the mathematical expression of (14) as follows:

$$\begin{aligned} &\min_U\ J_W(U)=\alpha J_1(U)+(1-\alpha)J_2(U)\\ &\text{s.t. } c_i(U)=0,\quad m_j(U)\le 0. \end{aligned} \tag{21}$$

Also simplify the mathematical expression of (18b) with the relaxation (20) as

$$\begin{aligned} &\min_U\ J_2(U)\\ &\text{s.t. } c_i(U)=0,\quad m_j(U)\le 0,\ J_1(U)\le\delta \end{aligned} \tag{22}$$

where $c_i(U)$ are the equality constraints including system dynamics and boundary conditions; $m_j(U)$ represent the inequality constraints including state constraints and control constraints; and $\delta=J_1^*(\xi)+\epsilon$.

Then we show the relationship between the two methods by explicating the KKT conditions.

Theorem 1: If the weights for the WS method are selected precisely the optimal values of dual variables for the LO method, the two methods yield the same optimal solution.

Proof: Let $\bar{J}_W(U)=\bar{\alpha}J_1(U)+J_2(U)$ with $\bar{\alpha}=\frac{\alpha}{1-\alpha}$. Obviously, to minimize J_W is equivalent to minimize $\bar{J}_W$. Define the Lagrangian for (21)

$$\bar{L}_W=J_2(U)+\Sigma\bar{\lambda}_i c_i(U)+\Sigma\bar{\mu}_j m_j(U)+\bar{\alpha}J_1(U)$$

where $\bar{\lambda}_i$ and $\bar{\mu}_j$ are dual variables.

Define the Lagrangian for (22)

$$L_\delta=J_2(U)+\Sigma\lambda_i c_i(U)+\Sigma\mu_j m_j(U)+\nu(J_1(U)-\delta)$$

where λ_i, μ_j and ν are dual variables. Then we list the detailed KKT conditions for (21) as follows:

$$\nabla_U\bar{L}_W(U^*)=0,\quad c_i(U^*)=0,\ m_j(U^*)\le 0 \tag{23a}$$
$$\bar{\mu}_j^* m_j(U^*)=0,\quad \bar{\mu}_j^*\ge 0 \tag{23b}$$

where ∇_U represents the gradient with respect to U. Let us also list the detailed KKT conditions for problem (22)

$$\nabla_U L_\delta(U^*)=0,\quad c_i(U^*)=0,\ m_j(U^*)\le 0 \tag{24a}$$
$$\mu_j^* m_j(U^*)=0,\quad \mu_j^*\ge 0 \tag{24b}$$
$$J_1(U^*)-\delta\le 0 \tag{24c}$$
$$\nu^*(J_1(U^*)-\delta)=0,\quad \nu^*\ge 0 \tag{24d}$$

Algorithm 2 (LO-MOMPC PF Algorithm)

1: Input the objective functions $J_i(U,\xi)$ in (12).
2: Measure current state $\xi(t)$.
3: Sequentially solve the lexicographic ordering subproblems (18) with $\xi=\xi(t)$.
4: Let $U^*=col(\omega_0^*,...,\omega_{N-1}^*)$ be the solution of the second layer problem (18b).
5: Implement ω_0^* for one sampling period.
6: At next time instant, set $t=t+\Delta t$; repeat from step 2.

Further expanding $\nabla_U \bar{L}_W(U^*)$ and $\nabla_U L_\delta(U^*)$, we have

$$\nabla J_2(U^*)+\Sigma\bar{\lambda}_i^*\nabla c_i(U^*)+\Sigma\bar{\mu}_j^*\nabla m_j(U^*)+\bar{\alpha}\nabla J_1(U^*)=0$$
$$\nabla J_2(U^*)+\Sigma\lambda_i^*\nabla c_i(U^*)+\Sigma\mu_j^*\nabla m_j(U^*)+\nu^*\nabla J_1(U^*)=0.$$

We notice that the main differences between the above two sets of KKT conditions are the presence of (24c) and (24d). But if $\bar{\alpha}=\nu^*$, (23) and (24) yield the same optimal solution U^* with $\bar{\lambda}_i^*=\lambda_i^*$ and $\bar{\mu}_j^*=\mu_j^*$ due to the fact that

Case 1: The last inequality is active, i.e., $J_1(U^*)=\delta$. Then (24c) and (24d) become solely $\nu^*\geq 0$. By definition we have $\bar{\alpha}\geq 0$, therefore, in this case the two sets of KKT conditions are exactly the same.

Case2: The last inequality is inactive, i.e., $J_1(U^*)<\delta$. Then (24c) and (24d) become $\nu^*=0$. So we have $\bar{\alpha}=\nu^*=0$, which make the two sets of KKT conditions identical. ■

Remark 2: Seen from the proof, the WS method and LO method are implicitly related by the optimal value of dual variables. Therefore, it is difficult to find the corresponding ϵ which generates the same solution as that using the WS method with the change of α obeying (15).

The LO-MOMPC algorithm is summarized in Algorithm 2.

V. Convergence Analysis

In order to follow the standard analysis procedure used in conventional MPC [25], the original MOMPC problem (11) needs to be modified and reformulated as the regulation problem of the error dynamics

$$\min_{\tilde{U}} \; J(\tilde{U},\tilde{\xi}) \tag{25a}$$
$$\text{s.t. } \tilde{\xi}_{k+1}=\tilde{h}(\tilde{\xi}_k,\tilde{\omega}_k),\quad \tilde{\xi}_0=\tilde{\xi}$$
$$\tilde{\xi}_k\in\tilde{\Xi},\quad k=1,2,\ldots,N$$
$$\tilde{\omega}_k\in\tilde{\Omega},\quad k=0,1,\ldots,N-1 \tag{25b}$$

where $\tilde{h}$ denotes the error dynamics; $J(\tilde{U},\tilde{\xi})=[J_1,J_2]^{\mathrm{T}}$ with $J_i=\sum_{k=0}^{N-1}L_i(\tilde{\xi}_k,\tilde{\omega}_k)+E_i(\tilde{\xi}_N)$; $\tilde{\Xi}$ and $\tilde{\Omega}$ denote system constraints.

Then the convergence of the solution for the MOMPC algorithm can be analyzed with the following assumptions.

Assumption 1: The functions $\tilde{h}(\cdot)$, $L_i(\cdot)$, and $E_i(\cdot)$ are continuous; $\tilde{h}(0,0)=0$, $L_i(0,0)=0$, and $E_i(0)=0$.

Assumption 2: The sets $\tilde{\Xi}$ and $\tilde{\Pi}$ are closed, and $\tilde{\Omega}$ is compact. Each set contains the origin in its interior.

Assumption 3: There exists an invariant set $\tilde{\Pi}$ for the error dynamics $\tilde{h}$, and a local controller $\kappa(\tilde{\xi})$ such that

$$\kappa(\tilde{\xi})\in\tilde{\Omega},\quad \tilde{h}(\tilde{\xi},\kappa(\tilde{\xi}))\in\tilde{\Pi},\ i=1,2$$
$$E_i(\tilde{h}(\tilde{\xi},\kappa(\tilde{\xi})))-E_i(\tilde{\xi})+L_i(\tilde{\xi},\kappa(\tilde{\xi}))\leq 0 \tag{26}$$

for any $\tilde{\xi}\in\tilde{\Pi}$.

For the WS-MOMPC scheme, we need to modify the problem by imposing the terminal constraints, i.e.,

$$J_W^*(\tilde{\xi},\alpha)=\min_{\tilde{U}}\{a^{\mathrm{T}}J(\tilde{U},\tilde{\xi})\mid (25b),\tilde{\xi}_N\in\tilde{\Pi}\}. \tag{27}$$

Also, before solving (27) a subproblem that determines the appropriate weight α has to be solved:

$$\alpha^*(\tilde{\xi},\alpha_d,J_\alpha)=\arg\min_{\alpha}\; f_\alpha(\alpha-\alpha_d) \tag{28a}$$
$$\text{s.t. } J_W^*(\tilde{\xi},\alpha)\leq J_\alpha$$
$$0\leq\alpha\leq 1 \tag{28b}$$

where α_d is the target weight calculated by (15); f_a is a convex function that measures the distance between α and α_d; Let $\tilde{U}_{-1}^*=\mathrm{col}(\tilde{\omega}_{-1,0}^*,\ldots,\tilde{\omega}_{-1,N-1}^*)$ and a_{-1}^* be the previous time solutions for (27) and (28), respectively. Then $J_\alpha=a_{-1}^{*\mathrm{T}}J(\tilde{U}^0,\tilde{\xi})$ with $\tilde{U}^0=\mathrm{col}(\tilde{\omega}_{-1,1}^*,\ldots,\tilde{\omega}_{-1,N-1}^*,\kappa(\tilde{\xi}_{-1,N}))$.

Theorem 2: Suppose *Assumptions 1–3* hold, and the problem (27) is feasible at time $t=0$. Then the error state converges to the origin, i.e., $\tilde{\xi}\to 0$ as $t\to\infty$.

Proof: The recursive feasibility is obtained since the shifted control sequence $\tilde{U}^0$ is always feasible for (27) and $a_{-1}^{*\mathrm{T}}$ is always feasible for (28) at the next time instant.

Evaluating the optimal value function of J_W^* at two successive time instants, we have

$$\begin{aligned}\Delta J_W &= J_W(\tilde{U}^*,\tilde{\xi})-J_W\left(\tilde{U}_{-1}^*,\tilde{\xi}_{-1,0}\right)\\ &= a^{*\mathrm{T}}J(\tilde{U}^*,\tilde{\xi})-a_{-1}^{*\mathrm{T}}J\left(\tilde{U}_{-1}^*,\tilde{\xi}_{-1,0}\right)\\ &\leq a_{-1}^{*\mathrm{T}}J(\tilde{U}^0,\tilde{\xi})-a_{-1}^{*\mathrm{T}}J\left(\tilde{U}_{-1}^*,\tilde{\xi}_{-1,0}\right)\\ &= \alpha_{-1}^*\big[E_1(\tilde{h}(\tilde{\xi}_{-1,N},\kappa(\tilde{\xi}_{-1,N})))-E_1(\tilde{\xi}_{-1,N})\\ &\quad+L_1(\tilde{\xi}_{-1,N},\kappa(\tilde{\xi}_{-1,N}))-L_1\left(\tilde{\xi}_{-1,0},\tilde{\omega}_{-1,0}^*\right)\big]\\ &\quad+\left(1-\alpha_{-1}^*\right)\big[E_2(\tilde{h}(\tilde{\xi}_{-1,N},\kappa(\tilde{\xi}_{-1,N})))-E_2(\tilde{\xi}_{-1,N})\\ &\quad+L_2(\tilde{\xi}_{-1,N},\kappa(\tilde{\xi}_{-1,N}))-L_2\left(\tilde{\xi}_{-1,0},\tilde{\omega}_{-1,0}^*\right)\big].\end{aligned}$$

By Assumption 3, $\Delta J_W\leq-\alpha_{-1}^*L_1(\tilde{\xi}_{-1,0},\tilde{\omega}_{-1,0}^*)-(1-\alpha_{-1}^*)L_2(\tilde{\xi}_{-1,0},\tilde{\omega}_{-1,0}^*)\leq 0$. By construction, we have $J_W\geq 0$. Therefore, $J_W^*(t)$ is a nonincreasing sequence and lower bounded by zero. By contradiction, we have $-\alpha_{-1}^*L_1(\tilde{\xi}_{-1,0},\tilde{\omega}_{-1,0}^*)-(1-\alpha_{-1}^*)L_2(\tilde{\xi}_{-1,0},\tilde{\omega}_{-1,0}^*)\to 0$ as $t\to\infty$. Since $Q_i>0$ and $R_i>0$ the convergence of the error state can be guaranteed, i.e., $\tilde{\xi}\to 0$ as $t\to\infty$. ■

For the LO-MOMPC PF scheme, the convergence of the solution can be guaranteed with the following assumption.

Assumption 4: There exist an invariant set $\tilde{\Pi}$ for the error dynamics $\tilde{h}$, containing the origin in the interior, and a local feedback control $\kappa_1(\tilde{\xi})$ such that

$$\kappa_1(\tilde{\xi})\in\tilde{\Omega},\quad \tilde{h}(\tilde{\xi},\kappa_1(\tilde{\xi}))\in\tilde{\Pi},$$
$$E_1(\tilde{h}(\tilde{\xi},\kappa_1(\tilde{\xi})))-E_1(\tilde{\xi})+L_1(\tilde{\xi},\kappa_1(\tilde{\xi}))\leq 0. \tag{29}$$

for any $\tilde{\xi}\in\tilde{\Pi}$.

We modify the LO-MOMPC problem by imposing the terminal constraints

$$J_1^*(\tilde{\xi}) = \min_{\tilde{U}}\{J_1(\tilde{U},\tilde{\xi}) \mid (25b), \tilde{\xi}_N \in \tilde{\Pi}\} \tag{30a}$$

$$J_2^*(\tilde{\xi}) = \min_{\tilde{U}} \left\{ J_2(\tilde{U},\tilde{\xi}) \middle| \begin{array}{c} J_1(\tilde{U},\tilde{\xi}) \le J_1^*(\tilde{\xi}) + \epsilon, \\ (25b), \quad \tilde{\xi}_N \in \tilde{\Pi} \end{array} \right\}. \tag{30b}$$

Theorem 3: Suppose *Assumptions 1, 2 and 4* hold, and for $\epsilon = 0$ the problem (30) is feasible at time $t = 0$. Let $\tilde{\xi}_{-1,0}$ denote the previous system state and $\tilde{\omega}^*_{-1,0}$ denote the first element of the previous time solution. For $t > 0$, if we choose $\epsilon = L_1(\tilde{\xi}_{-1,0}, \tilde{\omega}^*_{-1,0}) - \tilde{\xi}^{\mathrm{T}} Q_\epsilon \tilde{\xi}$ with $Q_1 > Q_\epsilon > 0$, then the error state converges to the origin, i.e., $\tilde{\xi} \to 0$ as $t \to \infty$.

Proof: Let $\tilde{U}^*_{-1} = \mathrm{col}(\tilde{\omega}^*_{-1,0}, \ldots, \tilde{\omega}^*_{-1,N-1})$ denote the previous time solution, and $\tilde{\xi}_{-1,i}$ denote the corresponding state prediction for $i = 0, 1, \ldots, N$. An initial guess $\tilde{U}^0 = \mathrm{col}(\tilde{\omega}^*_{-1,1}, \ldots, \tilde{\omega}^*_{-1,N-1}, \kappa_1(\tilde{\xi}_{-1,N}))$ can be constructed for the first layer subproblem (30a), which admits the horizontal feasibility. The hierarchical feasibility is also preserved since the solution of (30a) is always feasible for (30b).

Evaluating the optimal value function of J_1^* at these two successive sampling time instants, we have

$$\begin{aligned} \Delta J_1 &= J_1(\tilde{U}^*, \tilde{\xi}) - J_1(\tilde{U}^*_{-1}, \tilde{\xi}_{-1,0}) \\ &\le J_1(\tilde{U}^0, \tilde{\xi}) - J_1(\tilde{U}^*_{-1}, \tilde{\xi}_{-1,0}) + \epsilon \\ &= E_1(\tilde{h}(\tilde{\xi}_{-1,N}, \quad \kappa_1(\tilde{\xi}_{-1,N}))) - E_1(\tilde{\xi}_{-1,N}) \\ &\quad + L_1(\tilde{\xi}_{-1,N}, \quad \kappa_1(\tilde{\xi}_{-1,N})) - \tilde{\xi}^{\mathrm{T}} Q_\epsilon \tilde{\xi} \end{aligned} \tag{31}$$

With Assumption 4 we have $\Delta J_1 \le -\tilde{\xi}^{\mathrm{T}} Q_\epsilon \tilde{\xi} \le 0$. By construction, we know that $J_1 \ge 0$. Therefore, $J_1^*(t)$ is a nonincreasing sequence and lower bounded by zero. By contradiction, we have $-\tilde{\xi}^{\mathrm{T}} Q_\epsilon \tilde{\xi} \to 0$ as $t \to \infty$. Since $Q_\epsilon > 0$, the convergence of the error state trajectory to the origin can be guaranteed, i.e., $\tilde{\xi} \to 0$ as $t \to \infty$. ∎

Remark 3: There are different ways to reformulate the original PF problem as the regulation of the error dynamics and to satisfy the assumptions. As an example, we can take advantage of the ZPE manifold. Since the ZPE manifold (9a) serves as reference for the AUV to track, the following relation holds:

$$\begin{aligned} \dot{p}_x &= p_u \cos p_\psi - p_v \sin p_\psi \\ \dot{p}_y &= p_u \sin p_\psi + p_v \cos p_\psi \\ \dot{p}_\psi &= p_r. \end{aligned} \tag{32}$$

Decomposing the kinematic error $\tilde{\boldsymbol{\eta}}$ in the vessel parallel reference frame [23], we have

$$\tilde{\boldsymbol{\eta}} = \begin{bmatrix} \tilde{x} \\ \tilde{y} \\ \tilde{\psi} \end{bmatrix} = \begin{bmatrix} -\cos\psi & -\sin\psi & 0 \\ \sin\psi & -\cos\psi & 0 \\ 0 & 0 & -1 \end{bmatrix} \begin{bmatrix} x - p_x \\ y - p_y \\ \psi - p_\psi \end{bmatrix}.$$

Define the velocity error $\tilde{\mathbf{v}}$ in the following way:

$$\tilde{\mathbf{v}} = \begin{bmatrix} \tilde{u} \\ \tilde{v} \\ \tilde{r} \end{bmatrix} = \begin{bmatrix} u - p_u \cos\tilde{\psi} + p_v \sin\tilde{\psi} \\ v - p_u \sin\tilde{\psi} - p_v \cos\tilde{\psi} \\ r - p_r \end{bmatrix}.$$

Further define $\tilde{\boldsymbol{\tau}} = \mathrm{col}(\tilde{\tau}_1, \tilde{\tau}_2, \tilde{\tau}_3)$ in which

$$\begin{aligned} \tilde{\tau}_1 = {} & \frac{F_u}{M_{\dot{u}}} + \frac{M_{\dot{v}}}{M_{\dot{u}}}(\tilde{v} + p_u \sin\tilde{\psi} + p_v \cos\tilde{\psi})(\tilde{r} + p_r) \\ & - \frac{X_u}{M_{\dot{u}}}(\tilde{u} + p_u \cos\tilde{\psi} - p_v \sin\tilde{\psi}) \\ & - \frac{D_u}{M_{\dot{u}}}(\tilde{u} + p_u \cos\tilde{\psi} - p_v \sin\tilde{\psi})|\tilde{u} \\ & + p_u \cos\tilde{\psi} - p_v \sin\tilde{\psi}| \\ & - (\dot{p}_u \cos\tilde{\psi} + p_u \sin\tilde{\psi}\tilde{r} - \dot{p}_v \sin\tilde{\psi} + p_v \cos\tilde{\psi}\tilde{r}) \end{aligned} \tag{33}$$

$$\begin{aligned} \tilde{\tau}_2 = {} & \frac{F_v}{M_{\dot{v}}} - \frac{M_{\dot{u}}}{M_{\dot{v}}}(\tilde{u} + p_u \cos\tilde{\psi} - p_v \sin\tilde{\psi})(\tilde{r} + p_r) \\ & - \frac{Y_v}{M_{\dot{v}}}(\tilde{v} + p_u \sin\tilde{\psi} + p_v \cos\tilde{\psi}) \\ & - \frac{D_v}{M_{\dot{v}}}(\tilde{v} + p_u \sin\tilde{\psi} + p_v \cos\tilde{\psi})|\tilde{v} \\ & + p_u \sin\tilde{\psi} + p_v \cos\tilde{\psi}| \\ & - (\dot{p}_u \sin\tilde{\psi} - p_u \cos\tilde{\psi}\tilde{r} + \dot{p}_v \cos\tilde{\psi} + p_v \sin\tilde{\psi}\tilde{r}) \end{aligned} \tag{34}$$

$$\begin{aligned} \tilde{\tau}_3 = {} & \frac{F_r}{M_{\dot{r}}} - \frac{M_{\dot{v}} - M_{\dot{u}}}{M_{\dot{r}}}(\tilde{u} + p_u \cos\tilde{\psi} - p_v \sin\tilde{\psi}) \\ & \times (\tilde{v} + p_u \sin\tilde{\psi} + p_v \cos\tilde{\psi}) - \frac{N_r}{M_{\dot{r}}}(\tilde{r} + p_r) \\ & - \frac{D_r}{M_{\dot{r}}}(\tilde{r} + p_r)|\tilde{r} + p_r| - \dot{p}_r. \end{aligned} \tag{35}$$

Then it can be shown that

$$\dot{\tilde{\mathbf{x}}} = \begin{bmatrix} \dot{\tilde{x}} \\ \dot{\tilde{y}} \\ \dot{\tilde{\psi}} \\ \dot{\tilde{u}} \\ \dot{\tilde{v}} \\ \dot{\tilde{r}} \end{bmatrix} = \begin{bmatrix} p_r \tilde{y} - \tilde{u} + \tilde{y}\tilde{r} \\ -p_r \tilde{x} - \tilde{v} - \tilde{x}\tilde{r} \\ -\tilde{r} \\ \tilde{\tau}_1 \\ \tilde{\tau}_2 \\ \tilde{\tau}_3 \end{bmatrix} \triangleq \tilde{f}(\tilde{\mathbf{x}}, \tilde{\boldsymbol{\tau}}) \tag{36}$$

and at the origin $(\mathbf{0}, \mathbf{0})$, it admits that

$$\begin{aligned} \dot{p}_u &= \frac{M_{\dot{v}}}{M_{\dot{u}}} p_v p_r - \frac{X_u}{M_{\dot{u}}} p_u - \frac{D_u}{M_{\dot{u}}} p_u |p_u| + \frac{F_u}{M_{\dot{u}}} \\ \dot{p}_v &= -\frac{M_{\dot{u}}}{M_{\dot{v}}} p_u p_r - \frac{Y_v}{M_{\dot{v}}} p_v - \frac{D_v}{M_{\dot{v}}} p_v |p_v| + \frac{F_v}{M_{\dot{v}}} \\ \dot{p}_r &= \frac{M_{\dot{u}} - M_{\dot{v}}}{M_{\dot{r}}} p_u p_v - \frac{N_r}{M_{\dot{r}}} p_r - \frac{D_r}{M_{\dot{r}}} p_r |p_r| + \frac{F_r}{M_{\dot{r}}}. \end{aligned} \tag{37}$$

Comparing (32) and (37) with (1) and (2), we find that the ZPE manifold can be viewed as the state trajectory generated by a virtual AUV owning exact the same kinematic and dynamic properties as the real AUV. Since $(\mathbf{0}, \mathbf{0})$ indicates that the AUV is already on the manifold, the control F_u, F_v and F_r will make the AUV stay on the manifold.

Detailed derivation can be found in [15].

Define $\tilde{\xi} = \mathrm{col}(\tilde{\boldsymbol{\eta}}, \tilde{\mathbf{v}}, 0)$, $\tilde{\omega} = \mathrm{col}(\tilde{\boldsymbol{\tau}}, 0)$ and the error dynamics $\tilde{h} = \mathrm{col}(\tilde{f}, g)$. We modify J_1 with

$$L_1(\tilde{\xi}, \tilde{\omega}) = \|\tilde{\xi}\|^2_{Q_1} + \|\tilde{\omega}\|^2_{R_1}, \quad E_1(\tilde{\xi}) = \|\tilde{\xi}\|^2_{P_1}. \tag{38}$$

Leave L_2 and E_2 as in (13b). Notice that the error control signal construction (33)–(35) need the values of $\dot{p}_u$, $\dot{p}_v$ and $\dot{p}_r$.

By (9a), we have $\dot{p}_v = 0$ and the equations can be derived, as shown at the bottom of this page.

Since the above calculations require the information of $\ddot{s}$, the path dynamics is assigned a second-order integrator, i.e.,

$$\dot{z} = \tilde{A}z + \tilde{B}v_s, \quad \tilde{A} = \begin{bmatrix} 0 & 1 \\ 0 & 0 \end{bmatrix}, \quad \tilde{B} = \begin{bmatrix} 0 \\ 1 \end{bmatrix} \tag{39}$$

where $z = [s, \dot{s}]^{\mathrm{T}}$. Accordingly, the forward motion requirement will be formulated as $z_2 = \dot{s} \geq 0$. Further employ the manifold (9a) as the terminal constraint, i.e., $\tilde{\Pi} = \{0\}$. *Assumption 4* can be satisfied with $\kappa_1(0) = 0$.

VI. Simulation Studies

In this section, we present the simulation results of an AUV to follow a sinusoidal path $p_x(s) = s$ and $p_y(s) = \sin(s)$ with $s \geq 0$ in the local level plane. For the speed assignment, instead of directly setting a preferred path velocity $\dot{s}_r$, we set a desired surge velocity $u_r = 1$ [m/s] for the AUV. Then, according to (9a) and (10), we have the explicit expression

$$\dot{s}_r = u_r \left(p_x'^2 + p_y'^2\right)^{-\frac{1}{2}} \tag{40}$$

to calculate ξ_t at each sampling instant. The AUV parameters are extracted from the identified model of the Saab SeaEye Falcon based on [26]. The thrust limits $F_{u,\max} = 500$ [N], $F_{v,\max} = 500$ [N] and $F_{r,\max} = 500$ [Nm]. Initial conditions are $\mathbf{x}(0) = [0.5, 0, 0, 0, 0, 0]^{\mathrm{T}}$ and $s(0) = 0$.

A. Path-Following Control Using WS-MOMPC

For the WS-MOMPC PF control, the control parameters are selected as follows: $\Delta t = 0.1$, $N = 10$, $\gamma = 10^{-4}$, $K = I$, $Q_1 = \mathrm{diag}([10^5, 10^5, 10^2, 0.1, 0.1, 0.1, 0.1])$, $Q_2 = \mathrm{diag}([1, 1, 1, 10^3, 0.1, 0.1, 0.1])$, $P_1 = \mathrm{diag}([100, 100, 10, 10^{-3}, 10^{-3}, 10^{-3}, 10^{-3}])$, $P_2 = \mathrm{diag}([0.1, 0.1, 0.1, 100, 10^{-3}, 10^{-3}, 10^{-3}])$, and $R_1 = R_2 = \mathrm{diag}([10^{-3}, 10^{-3}, 10^{-3}, 10^{-3}])$.

The AUV PF results with different β values are shown in Fig. 1. It can be observed that 1) for all of the three cases, the AUV trajectory successfully converges to the desired sinusoidal path, which validates the effectiveness of the proposed WS-MOMPC PF method; 2) for each case, at the beginning the AUV moves in the direction that is almost perpendicular to the path in order to get the fastest convergence; and 3) the larger β value results in faster path convergence because the β value accounts for the sensitivity (slope) of the logistic function.

Fig. 2 records the surge velocity of the AUV during the simulation (for the case of $\beta = 1$).

As we can see, the surge velocity keeps very well at the desired speed after the sacrifice for path convergence in the beginning. In Fig. 3, the AUV thrust forces and moments as well as the imaginary path control input are plotted. As expected, they are all within the corresponding ranges of permitted values, which validate the effectiveness of barrier functions in the PMP implementation.

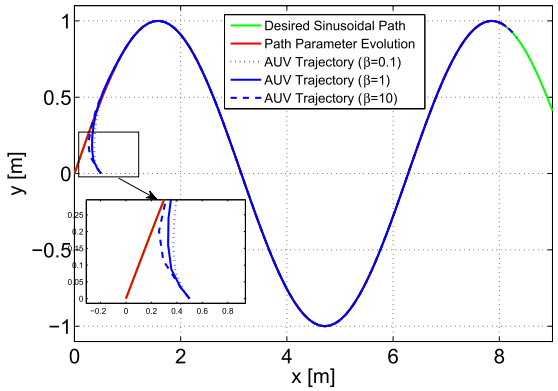

Fig. 1. PF results using WS-MOMPC.

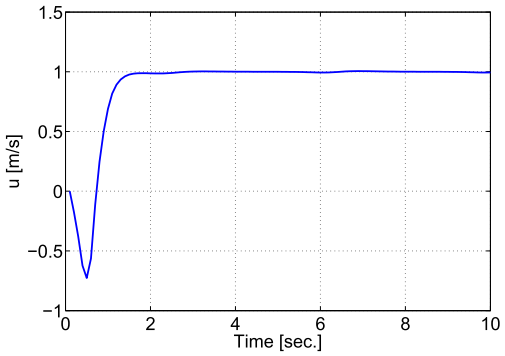

Fig. 2. Surge velocity of the AUV (WS-MOMPC).

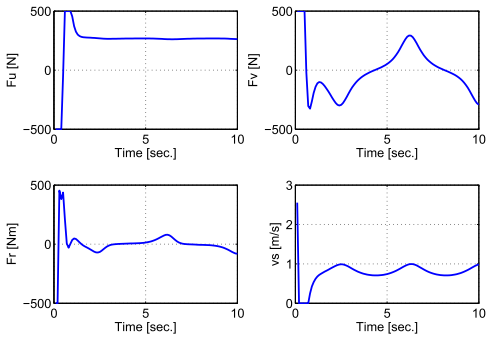

Fig. 3. Control inputs of the augmented system (WS-MOMPC).

B. Path-Following Control Using LO-MOMPC

For the LO-MOMPC scheme, the control parameters are selected as follows: $\Delta t = 0.1$, $N = 10$, $Q_1 = \mathrm{diag}([10^5, 10^5, 10^3, 10^3, 10^{-3}, 10^{-3}, 10^{-3}])$,

$$\dot{p}_u = \left(p_x' p_x'' + p_y' p_y''\right)\left(p_x'^2 + p_y'^2\right)^{-\frac{1}{2}}\dot{s}^2 + \left(p_x'^2 + p_y'^2\right)^{\frac{1}{2}}\ddot{s}$$

$$\dot{p}_r = \frac{\left(p_x'^2 + p_y'^2\right)\left(p_x' p_y''' - p_y' p_x'''\right) - 2\left(p_x' p_y'' - p_y' p_x''\right)\left(p_x' p_x'' + p_y' p_y''\right)}{\left(p_x'^2 + p_y'^2\right)^2}\dot{s}^2 + \frac{p_x' p_y'' - p_y' p_x''}{p_x'^2 + p_y'^2}\ddot{s}$$

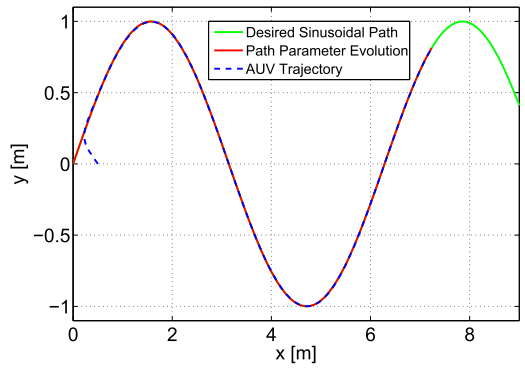

Fig. 4. PF results using LO-MOMPC.

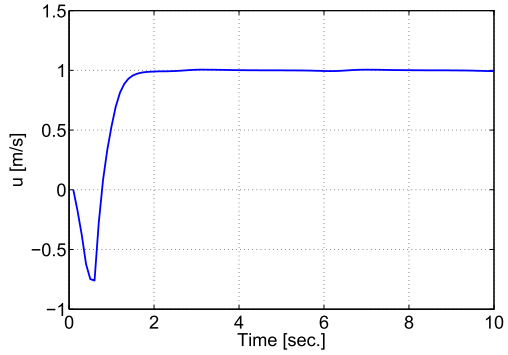

Fig. 5. Surge velocity of the AUV (LO-MOMPC).

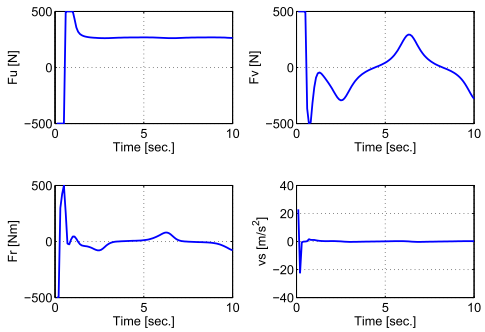

Fig. 6. Control inputs of the augmented system (LO-MOMPC).

$Q_2 = \text{diag}([10^4, 10^4, 10^2, 10^3, 10^{-3}, 10^{-3}, 10^3])$, $P_1 = \text{diag}([100, 100, 10, 100, 10^{-3}, 10^{-3}, 10^{-3}])$, $P_2 = \text{diag}([100, 100, 10, 100, 10^{-3}, 10^{-3}, 10^2])$ $R_1 = R_2 = \text{diag}([10^{-3}, 10^{-3}, 10^{-3}, 10^{-3}])$.

The AUV PF results are shown in Fig. 4. Similar observations can be made: 1) the AUV trajectory successfully converge to the desired sinusoidal path, which validates the effectiveness of the proposed LO-MOMPC PF method and 2) in the beginning, the AUV moves in the direction almost perpendicular to the desired path in order to get the fastest convergence, which reflects the prioritization of the two objectives. Fig. 5 records the surge velocity of the AUV during the simulation.

The surge velocity keeps very well at the desired speed after the initial sacrifice for path convergence. In Fig. 6, the AUV thrust forces and moments as well as the imaginary path control input are plotted.

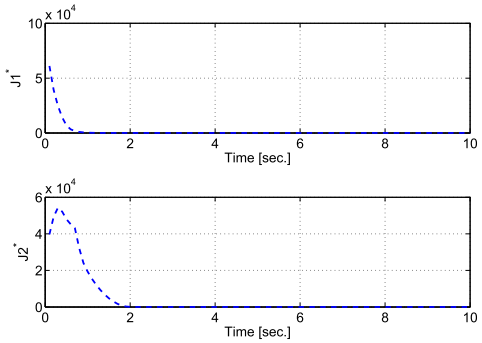

Fig. 7. Optimal value functions.

Also the optimal value functions are plotted in Fig. 7. It can be seen that J_1^* decreases monotonically, which reflects that the path convergence can be obtained; while J_2^* admits an initial hike before dropping, which conforms to the strict prioritization of the objectives.

VII. Conclusion

In this brief, the PF problem of an AUV was studied. Considering the prioritization in the PF requirements, we have developed the MOMPC framework along with the WS-MOMPC algorithm and the LO-MOMPC algorithm. The relation between the two proposed methods was explored and the sufficient conditions that guarantee the convergence of the solution were derived. Simulation results on the Falcon AUV revealed the effectiveness. In the near future, the robustness of the proposed MOMPC method will be explicitly investigated and the incorporation of incremental input constraints will be considered for real-world PF applications.

References

[1] W. Caharija *et al.*, "Integral line-of-sight guidance and control of underactuated marine vehicles: Theory, simulations, and experiments," *IEEE Trans. Control Syst. Technol.*, vol. 24, no. 5, pp. 1623–1642, Sep. 2016.

[2] X. Xiang, C. Yu, and Q. Zhang, "Robust fuzzy 3D path following for autonomous underwater vehicle subject to uncertainties," *Comput. Operat. Res.*, vol. 84, pp. 165–177, Aug. 2017.

[3] J. Miao, S. Wang, Z. Zhao, Y. Li, and M. Tomovic, "Spatial curvilinear path following control of underactuated AUV with multiple uncertainties," *ISA Trans.*, vol. 67, pp. 107–130, Mar. 2017.

[4] A. Micaelli and C. Samson, "Trajectory tracking for a unicycle-type and two steering wheels mobile robots," INRIA, Sophia-Antipolis, Nice, France, Tech. Rep. 2097, 1993.

[5] P. Encarnacao and A. Pascoal, "3D path following for autonomous underwater vehicle," in *Proc. 39th IEEE Conf. Desicion Control*, Sydney, NSW, Australia, Dec. 2000, pp. 2977–2982.

[6] P. Encarnacao, A. Pascoal, and M. Arcak, "Path-following for marine vehicles in the presence of unknown currents," in *Proc. 6th IFAC Symp. Robot Control*, Vienna, Austria, 2000, pp. 469–474.

[7] L. Lapierre and D. Soetanto, "Nonlinear path-following control of an AUV," *Ocean Eng.*, vol. 34, nos. 11–12, pp. 1734–1744, 2007.

[8] L. Lapierre and B. Jouvencel, "Robust nonlinear path-following control of an AUV," *IEEE J. Ocean. Eng.*, vol. 33, no. 2, pp. 89–102, Apr. 2008.

[9] T. Faulwasser, B. Kern, and R. Findeisen, "Model predictive path-following for constrained nonlinear systems," in *Proc. 48th IEEE Conf. Decision Control*, Shanghai, China, Dec. 2009, pp. 8642–8647.

[10] T. Faulwasser and R. Findeisen, "Constrained output path-following for nonlinear systems using predictive control," in *Proc. 8th IFAC Symp. Nonlinear Control Syst.*, Bologna, Italy, 2010, pp. 753–758.

[11] M. Böck and A. Kugi, "Real-time nonlinear model predictive path-following control of a laboratory tower crane," *IEEE Trans. Control Syst. Tech.*, vol. 22, no. 4, pp. 1461–1474, Jul. 2014.
[12] A. Pavlov, H. Nordahl, and M. Breivik, "MPC-based optimal path following for underactuated vessels," in *Proc. 8th IFAC Int. Conf. Manoeuving Control Marine Craft*, Guaruja, Brazil, 2009, pp. 340–345.
[13] S. Oh and J. Sun, "Path following of underactuated marine surface vessels using line-of-sight based model predictive control," *Ocean Eng.*, vol. 37, no. 2, pp. 289–295, 2010.
[14] A. Alessandretti, A. P. Aguiar, and C. N. Jones, "Trajectory-tracking and path-following controllers for constrained underactuated vehicles using model predictive control," in *Proc. Eur. Control Conf.*, Zürich, Switzerland, 2013, pp. 1371–1376.
[15] C. Shen, Y. Shi, and B. Buckham, "Integrated path planning and tracking control of an AUV: A unified receding horizon optimization approach," *IEEE/ASME Trans. Mechatronics*, vol. 22, no. 3, pp. 1163–1173, Jun. 2017.
[16] C. Shen, B. Buckham, and Y. Shi, "Modified C/GMRES algorithm for fast nonlinear model predictive tracking control of AUVs," *IEEE Trans. Control Syst. Tech.*, vol. 25, no. 5, pp. 1896–1904, Sep. 2017.
[17] C. Ocampo-Martinez, A. Ingimundarson, V. Puig, and J. Quevedo, "Objective prioritization using lexicographic minimizers for MPC of sewer networks," *IEEE Trans. Control Syst. Tech.*, vol. 16, no. 1, pp. 113–121, Jan. 2008.
[18] D. Zambrano and E. F. Camacho, "Application of MPC with multiple objective for a solar refrigeration plant," in *Proc. IEEE Conf. Control Appl.*, Glasgow, Scotland, Sep. 2002, pp. 1230–1235.
[19] A. Bemporad and D. M. de la Peña, "Multiobjective model predictive control," *Automatica*, vol. 45, no. 12, pp. 2823–2830, 2009.
[20] V. Zavala and A. Flores-Tlacuahuac, "Stability of multiobjective predictive control: A utopia-tracking approach," *Automatica*, vol. 48, no. 10, pp. 2627–2632, Oct. 2012.
[21] D. He, L. Wang, and J. Sun, "On stability of multiobjective NMPC with objective prioritization," *Automatica*, vol. 57, pp. 189–198, Jul. 2015.
[22] M. A. Müller and F. Allgöwer, "Improving performance in model predictive control: Switching cost functionals under average dwell-time," *Automatica*, vol. 48, no. 42, pp. 402–409, 2012.
[23] T. I. Fossen, *Marine Control Systems: Guidance, Navigation and Control of Ships, Rigs and Underwater Vehicles*. Trondheim, Norway: Marine Cybernetics, 2002.
[24] K. Graichen, "A fixed-point iteration scheme for real-time model predictive control," *Automatica*, vol. 48, no. 7, pp. 1300–1305, 2012.
[25] J. Rawlings, D. Mayne, and M. M. Diehl, *Model Predictive Control: Theory, Computation, and Design*. Madison, WI, USA: Nob Hill Publishing, 2009.
[26] A. A. Proctor, "Semi-autonomous guidance and control of a Saab SeaEye Falcon ROV," Ph.D. dissertation, Dept. Mech. Eng., Univ. Victoria, Victoria, BC, USA, 2014.